

## SPECIAL PROJECT FINAL REPORT

All the following mandatory information needs to be provided.

<b>Project Title:</b>	Sensitivity experiments on decadal prediction
<b>Computer Project Account:</b>	SPITMECC
<b>Start Year - End Year :</b>	2019 - 2021
<b>Principal Investigator(s)</b>	Virna Loana Meccia
<b>Affiliation/Address:</b>	Institute of Atmospheric Sciences and Climate, National Research Council (ISAC-CNR), Italy.
<b>Other Researchers (Name/Affiliation):</b>	ISAC-CNR: S. Corti, J. von Hardenberg, P. Davini, F. Fabiano

The following should cover the entire project duration.

## **Summary of project objectives**

(10 lines max)

The original Special Project (SP) aimed to explore the role of ocean decadal variability on global climate. We aimed to focus on how the North Atlantic and North Pacific sea surface temperatures modulate the global surface temperature trends and the regional climate variability in Europe. The original plan was to apply EC-Earth to a series of experiments designed following the Decadal Climate Prediction Project.

## **Summary of problems encountered**

(If you encountered any problems of a more technical nature, please describe them here.)

Motivated by recent results at the beginning of this SP, we have considered it of utmost importance to deviate from the original plan to study the impacts of including Stochastic Physics Schemes (SPS) in the atmospheric component of EC-Earth on the predicted climate. In this context, we have started a collaboration with the University of Oxford, and we used the computing resources of the first two years of this SP to address open questions regarding the impacts of including SPS in EC-Earth on Climate Sensitivity.

We used the computing resources of the third year of this SP to complete a set of long simulations in which a quasi-equilibrium state is reached under different greenhouse gas concentrations. In particular, the simulation run with this project helped to assess the multi-centennial AMOC variability found under pre-industrial conditions in a warmer climate. A paper in this is currently under review on Climate Dynamics.

## **Experience with the Special Project framework**

(Please let us know about your experience with administrative aspects like the application procedure, progress reporting etc.)

The experience with the application and submission has been straightforward. Besides, the staff at ECMWF helped assist with any problems, in particular when I needed extra space to deal with model outputs.

## **Summary of results**

(This section should comprise up to 10 pages, reflecting the complexity and duration of the project, and can be replaced by a short summary plus an existing scientific report on the project.)

As explained above, the resources of this SP were used to deepen the study of the following two scientific topics: a) the climate impacts of including Stochastic Physics Schemes (SPS) in the atmospheric component of EC-Earth, and b) the multi-centennial variability of the Atlantic Meridional Overturning Circulation (AMOC) simulated by EC-Earth in a warmer climate. In what follows, we report the summary of results regarding these two lines of investigation.

## a) Climate impacts of including Stochastics Physics Scheme in the atmospheric component of EC-Earth

### a.1) Part I: Stochastic Parameterizations and the climate response to external forcing: an experiment with EC-Earth

We analysed the potential effects of including SPS in the atmospheric component of the EC-Earth climate model on the evolution of the sea-ice extent in the Arctic during long-term simulations covering the historical and future periods.

The experiments analysed in the beginning are part of the Climate Stochastic Physics High-resolutionN eXperiments (Climate SPHINX) project which aimed at evaluating the impact of model resolution and stochastic parameterizations on the simulated climate (for details, see Davini et al., 2017). Simulations were carried out using version 3.1 of the EC-Earth climate model (Hazeleger et al., 2010, 2012). In particular, we used six coupled climate simulations: three ensemble members that constitute the control runs (*base*) and three ensemble members that include SPS (*stoc*). For the latter, both the Stochastically Perturbed Parameterization Tendencies (SPPT) scheme (Buizza et al., 1999) and the Stochastic Kinetic Energy Backscatter (SKEB) scheme (Palmer et al., 2009) are incorporated into the atmospheric component of EC-Earth. SPHINX simulations span from 1850 to 2100. Because we have found that the most interesting response occurred around the year 2100, using the computing resources of the first year of this SP, we extended each run for 60 years using the same model code and configuration as in Davini et al. (2017). The RCP8.5 setup has been followed for the greenhouse gas emissions, while the ozone values of the year 2100 were kept constant during the extended period. In this way, six 310-year (1850–2160) simulations have been analysed.

The simulated Arctic sea-ice extent in September and March (Fig. 1) displays an overall decrease. The sea-ice loss is faster in the *base* experiments than in the *stoc* ones. An Arctic free of sea ice (less than  $1 \times 10^6$  km<sup>2</sup> of sea-ice extent for at least five consecutive years) in September occurs around 2075 for the *base* experiments and around 2083 for the *stoc* ones (Table 1; Fig. 1a). In all the experiments, the model simulates an abrupt sea-ice loss in March (Fig. 1b). It occurs about ten years earlier in the *base* experiments than in the *stoc* ones (Table 1; Fig. 1b). An Arctic free of sea ice in March occurs at around 2151 in the *base* runs and 2153 in the *stoc* runs (Table 1). The evolution of the global annual mean surface air temperature (GSAT; Fig. 1c) is similar among the ensemble members but differs if the stochastic physics is on or off. Curves start separating by the second half of the 20th century; the difference results maximum in 2100, and curves become almost indistinguishable between both sets of experiments around 2110. This result is confirmed by Fig. 1d, which shows the difference in temperature with respect to the *base* ensemble mean. The largest difference between the *base* and *stoc* runs is around 2100.

	<i>Base ensemble mean</i>	<i>Stoc ensemble mean</i>
Arctic free of sea ice in September (yr)	~ 2075	~ 2083
Abrupt loss of sea ice in March (yr)	~ 2093	~ 2104
Arctic free of sea ice in March (yr)	~ 2151	~ 2153

Table 1. Summary of the differences between the *base* and *stoc* experiments in simulating the evolution of Arctic sea ice.

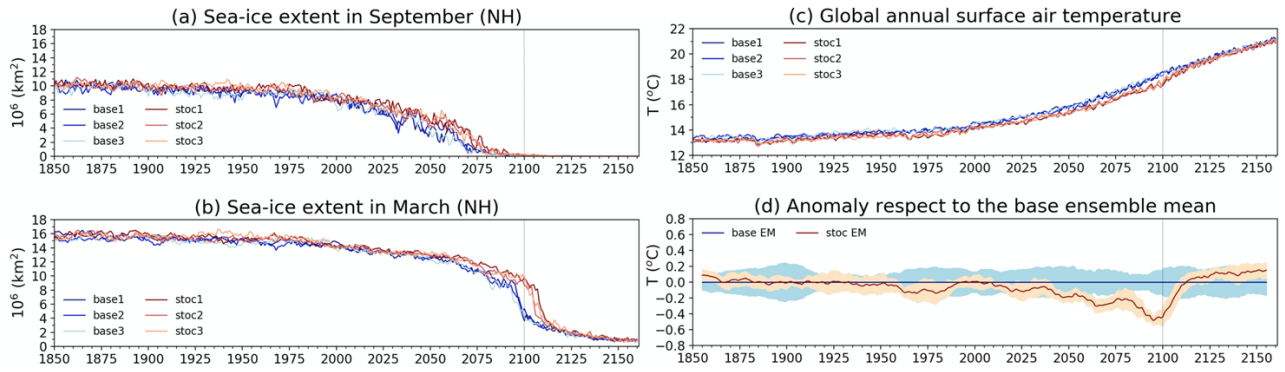


Figure 1: Results of the simulations from 1850 to 2160. NH sea-ice extent in (a) September and (b) March; (c) GSAT ( $^{\circ}\text{C}$ ) and (d) difference with respect to the base ensemble mean of the GSAT increment ( $^{\circ}\text{C}$ ). Ten-year moving averaged ensemble means and the ensemble members' spreads are plotted in (d). All three ensemble members for the base and stoc experiments are plotted in blue and red, respectively. The grey vertical line indicates when the original runs end and the extended simulations start.

It is apparent that the transient climate sensitivity is lower when the SPS are activated only during the 21st century. Curiously, the situation reverses at the beginning of the 22nd century, coinciding with the simulated free sea ice conditions in the Arctic throughout the year. Strommen et al. (2019) have associated the smaller transient climate sensitivity of the *stoc* runs with changes in the low-level cloud cover (LCC) feedback. LCC versus the GSAT is plotted in Fig. 2a. Blue dots are associated with the *base* ensemble mean, whereas the *stoc* ensemble mean is shown as red dots. In both experiments, LCC decreases when GSAT increases up to a value of about  $18.5^{\circ}\text{C}$ , which occurs shortly after the year 2100 (Fig. 1c). The LCC response to global warming represents a positive feedback for the system (Bony et al., 2015), which is larger in the *base* runs until 2100, yielding a larger temperature increase. However, the LCC positive feedback is much weaker after the year 2100 for the two sets of experiments and does not explain the differences in the two responses. The larger energy imbalance of the *stoc* runs is explained by lower upward thermal radiation at the top of the atmosphere (not shown). This can be associated with an increase in the area covered by high-level clouds (HCC), which reflect little sunlight, but since they have a low emission temperature, they warm the surface more than they cool it (section 7.2.1.2 in Boucher et al., 2013). The relation between HCC and GSAT is shown in Fig. 2b. For GSAT lower than  $\sim 17^{\circ}\text{C}$ , higher values of HCC are found in the *base* runs. However, when GSAT crosses this threshold value, the HCC level in the *stoc* experiments equals that in the *base* ones, and the derivative of the red curve in Fig. 2b becomes positive. This leads to enhanced production of HCC with temperatures higher than  $17^{\circ}\text{C}$ , which in turn contributes to a further increase in warming (positive feedback). This positive feedback in the *stoc* runs triggers the sudden temperature increment (Fig. 1c).

The interaction between the random perturbations in temperature or humidity (introduced by the inclusion of SPS) with the process of condensation of an air parcel close to saturation can explain the behaviour mentioned above. For instance, we found that the global surface relative humidity increases with warming (Fig. 2c), going from 74% to 76%. This increment is simulated in all the runs, it is roughly linear for temperatures higher than  $\sim 17^{\circ}\text{C}$ , and it is similar for both sets of experiments, *base* and *stoc*. So, it is possible that once a certain critical threshold of relative humidity is achieved, SPS foster the development of convective events. Indeed, there is a strong relationship between the HCC and the surface relative humidity (Fig. 2d).

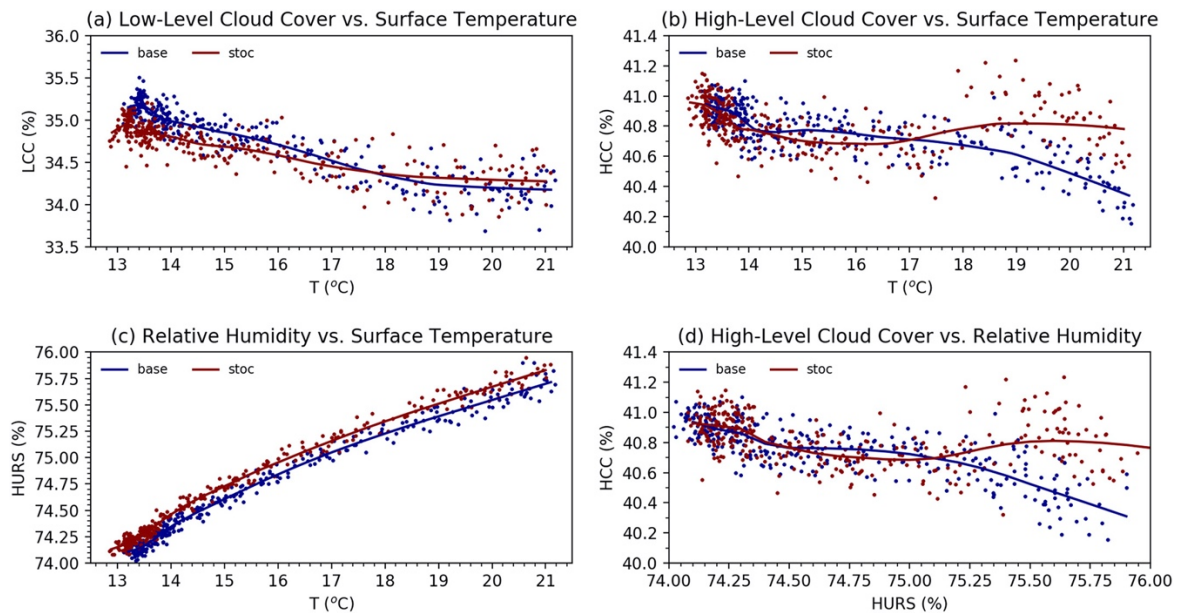


Figure 2: Globally averaged (a) LCC; (b) HCC and (c) surface relative humidity (HURS) versus the GSAT; and (d) HCC versus HURS for the ensemble mean of the base (blue) and stoc (red) experiments. Solid lines are the results of a nonparametric regression method (locally estimated scatterplot smoothing).

It is worth noting that the regime shift occurs at about the same GSAT value that the one which represents the threshold value for the abrupt collapse of winter sea ice in the Arctic. Although the timing of these two dramatic shifts (i.e., the abrupt decline of winter sea ice and the swift high-level clouds formation) is remarkable, there is no evident physical mechanism that could tie the two processes. The two abrupt changes might be independent responses to a given level of global warming. In conclusion, including SPS in EC-Earth yields differences not only in the simulated mean climate but also in the path that the model travels along its phase space to achieve it.

These results from section a.1) were published in Geophysical Research Letters in 2020, and the SP SPITMECC was acknowledged (Meccia et al., 2020).

### ***a.2) Part II: Impacts of the Stochastics Physics Scheme inclusion in the atmospheric component of EC-Earth on Climate Sensitivity***

By analysing the simulations run with the computing time of the first year, we have found that the impacts of including SPS in EC-Earth on the transient climate sensitivity are highly dependent on the mean state of the climate. In light of this result, we used the computing resources of the second year of this SP to perform climate simulations oriented to better understand the impacts of SPS on climate sensitivity. We have applied the SPS on the CMIP6-generation EC-Earth climate model to a *spin-up*, a *piControl* and an *abrupt4xCO2* experiments. In particular, with the resources of this SP we run ~170 years of the *abrupt4xCO2* experiment in which the SPS were activated in EC-Earth3 (EC-Earth3S). This run, together with the *piControl* experiment (also with the SPS activated), allows us to compute the Equilibrium Climate Sensitivity (ECS) and to compare the result with the ECS obtained for the equivalent CMIP6 experiments with the standard EC-Earth3, in which the SPS are not activated (EC-Earth3). Climate sensitivity is typically defined as the global temperature rise following a doubling of CO<sub>2</sub> concentration in the atmosphere compared to pre-industrial levels. The ECS is, therefore, the temperature increase that would eventually occur (after hundreds or even thousands of years) when the climate system fully adjusts to a sustained doubling of CO<sub>2</sub>.

The timeseries of global air surface temperature (TAS) for four experiments (*piControl* and *abrupt4xCO2*, both with EC-Earth3 and EC-Earth3S) are plotted in Fig. 3. The ECS was computed by applying the method of Gregory et al. (2004). As models may present an energy balance that is not

perfectly closed, resulting in a nonzero equilibrium at the Top of the Atmosphere (TOA) net flux (Qnet), the *piControl* equilibrium values are typically removed from the *abrupt4xCO2* values before proceeding with the computation of ECS. To do so, we subtracted from the *abrupt4xCO2* experiment values the mean values of both, Qnet and TAS of the corresponding *piControl* experiment. We plotted the increments in Qnet versus the increments in TAS with respect to the equilibrium *piControl*, and we fitted a line to the scatterplots (Fig. 4). The fitted line gives us information about the ECS (intercept of the linear fit with the abscissa divided by 2), the radiative feedback parameter (slope) and the effective radiative forcing (ERF; intercept with the ordinate divided by 2), as shown in Table 2. Although previous studies show that the inclusion of SPS affects the transient climate sensitivity (Strommen et al, 2019; Meccia et al., 2020), the ECS is similar in both cases, EC-Earth3 and EC-Earth3S. In collaboration with Kristian Strommen from the University of Oxford, we are still investigating this issue, and we are preparing a paper.

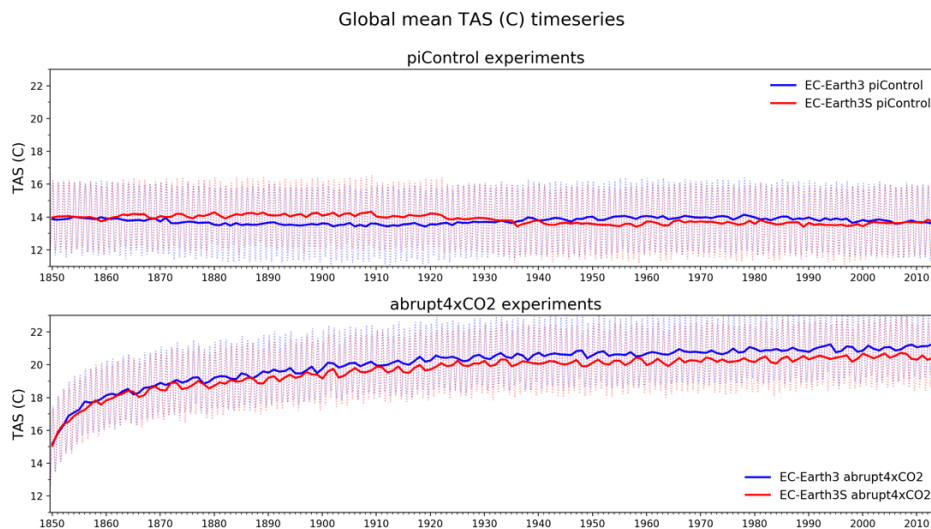


Figure 3. Timeseries of monthly and annual TAS (°C) for the *piControl* (upper panel) and *abrupt4xCO2* (lower panel). Blue lines correspond to the runs without the SPS activated in the atmospheric component whereas red lines correspond to the experiments with the SPS activated.

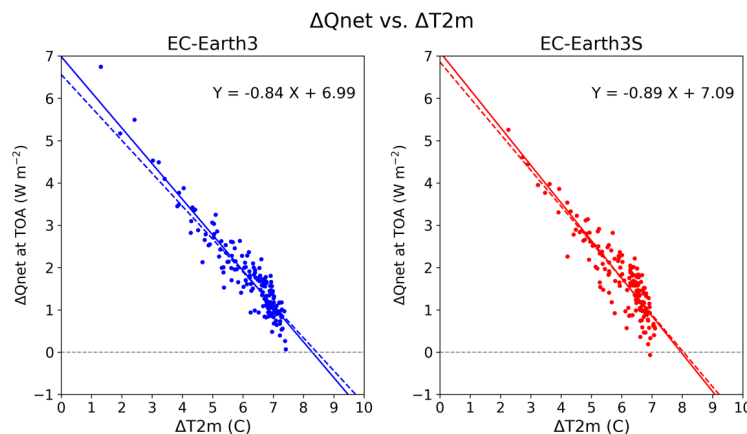


Figure 4: Gregory plots from the *abrupt4xCO2* experiment of EC-Earth3 without (left) and with (right) the SPS activated in the atmospheric component after subtracting the corresponding *piControl* equilibrium value. A regression line considering all the data (solid line) and the last 155 years (dashed line) is fitted.

MODEL	ECS	$\lambda$	ERF
EC-Earth3	4.14	-0.84	3.49
EC-Earth3S	3.98	-0.89	3.54

Table 2. Equilibrium climate sensitivity (ECS, in  $^{\circ}\text{C}$ ), net feedback parameter ( $\lambda$ , in  $\text{W m}^{-2} \text{K}^{-1}$ ) and effective radiative forcing (ERF, in  $\text{W m}^{-2}$ ) in EC-Earth3 and EC-Earth3S.

## References

- Bony S., Stevens B., Frierson D.M., Jakob C., Kageyama M., Pincus R., Shepherd T.G., Sherwood S.C., Siebesma A.P., Sobel A.H. and Watanabe M. (2015). Clouds, circulation and climate sensitivity. *Nature Geoscience*, 8(4), 261– 268. <https://doi.org/10.1038/ngeo2398>
- Boucher O., Randall D., Artaxo P., Bretherton C., Feingold G., Forster P., Kerminen V.-M., Kondo Y., Lia H., Lohmann U., Rasch P., Satheesh S.K., Sherwood S., Stevens B. and Zhang X.Y. (2013). In *Climate Change 2013: The Physical Science Basis*. In T.F. Stocker, D. Qin, G.-K. Plattner, M. Tignor, S.K. Allen, J. Doschung, A. Nauels, Y. Xia, V. Bex, and P.M. Midgley (Eds.), Contribution of Working Group I to the Fifth Assessment Report of the Intergovernmental Panel on Climate Change. United Kingdom and New York, NY, USA: Cambridge University Press. pp. 571- 657. <https://doi.org/10.1017/CBO9781107415324.016>
- Buizza R., Miller M. and Palmer T.N. (1999). Stochastic representation of model uncertainties in the ECMWF ensemble prediction system. *Quarterly Journal of the Royal Meteorological Society*, 125, 2887– 2908. <https://doi.org/10.1002/qj.49712556006>
- Davini P., von Hardenberg J., Corti S., Christensen H.M., Juricke S., Subramanian A., Watson P.A.G., Weisheimer A. and Palmer T.N. (2017). Climate SPHINX: evaluating the impact of resolution and stochastic physics parameterisations in the EC-Earth global climate model. *Geoscientific Model Development*, 10(3), 1383– 1402. <https://doi.org/10.5194/gmd-10-1383-2017>
- Gregory J.M., Ingram W.J., Palmer M.A., Jones G.S., Stott P.A., Thorpe R.B., Lowe J.A., Johns T.C. and Williams K.D. (2004). A new method for diagnosing radiative forcing and climate sensitivity. *Geophysical Research Letters*, 31, L03205. <https://doi.org/10.1029/2003GL018747>
- Hazeleger W., Severijns C., Semmler T., Ștefănescu S., Yang S., Wang X., Wyser K., Dutra E., Baldasano J.M., Bintanja R. and Bougeault P. (2010). EC-Earth: A seamless Earth-system prediction approach in action. *Bulletin of the American Meteorological Society*, 91(10), 1357– 1364. <https://doi.org/10.1175/2010BAMS2877.1>
- Hazeleger W., Wang X., Severijns C., Ștefănescu S., Bintanja R., Sterl A., Wyser K., Semmler T., Yang S., van den Hurk B., van Noije T., van der Linden E. and van der Wiel K. (2012). EC-Earth V2.2: description and validation of a new seamless Earth system prediction model. *Climate Dynamics*, 39(11), 2611– 2629. <https://doi.org/10.1007/s00382-011-1228-5>
- Meccia V.L., Fabiano F., Davini P. and Corti S. (2020). Stochastic parameterizations and the climate response to external forcing: An experiment with EC-Earth. *Geophysical Research Letters*, 47, e2019GL085951. <https://doi.org/10.1029/2019GL085951>.
- Palmer T.N., Buizza R., Doblas-Reyes F., Jung T., Leutbecher M., Shutts G.J., Steinheimer M., Weisheimer A. (2009). Stochastic parametrization and model uncertainty. ECMWF Technical Report 598, 44 pp. [Available online at <https://www.ecmwf.int/en/elibrary/11577-stochastic-parametrization-and-model-uncertainty>].
- Strommen K., Watson P.A.G. and Palmer T.N. (2019). The impact of a stochastic parameterization scheme on climate sensitivity in EC-Earth. *Journal of Geophysical Research- Atmosphere*, 124. <https://doi.org/10.1029/2019JD030732>

## b) Multi-centennial AMOC variability in EC-Earth

It has been shown that the *piControl* run of the CMIP6 generation EC-Earth climate model is dominated by a multi-centennial variability of the Atlantic Meridional Overturning Circulation (AMOC). In particular, the AMOC in the *piControl* run with EC-Earth3 is dominated by a fluctuation of about 150 years (Fig. 5c). The amplitude of these oscillations (black line in Fig. 5a) is larger than the amplitude of the inter-annual to multi-decadal variability (grey line in Fig. 5a).

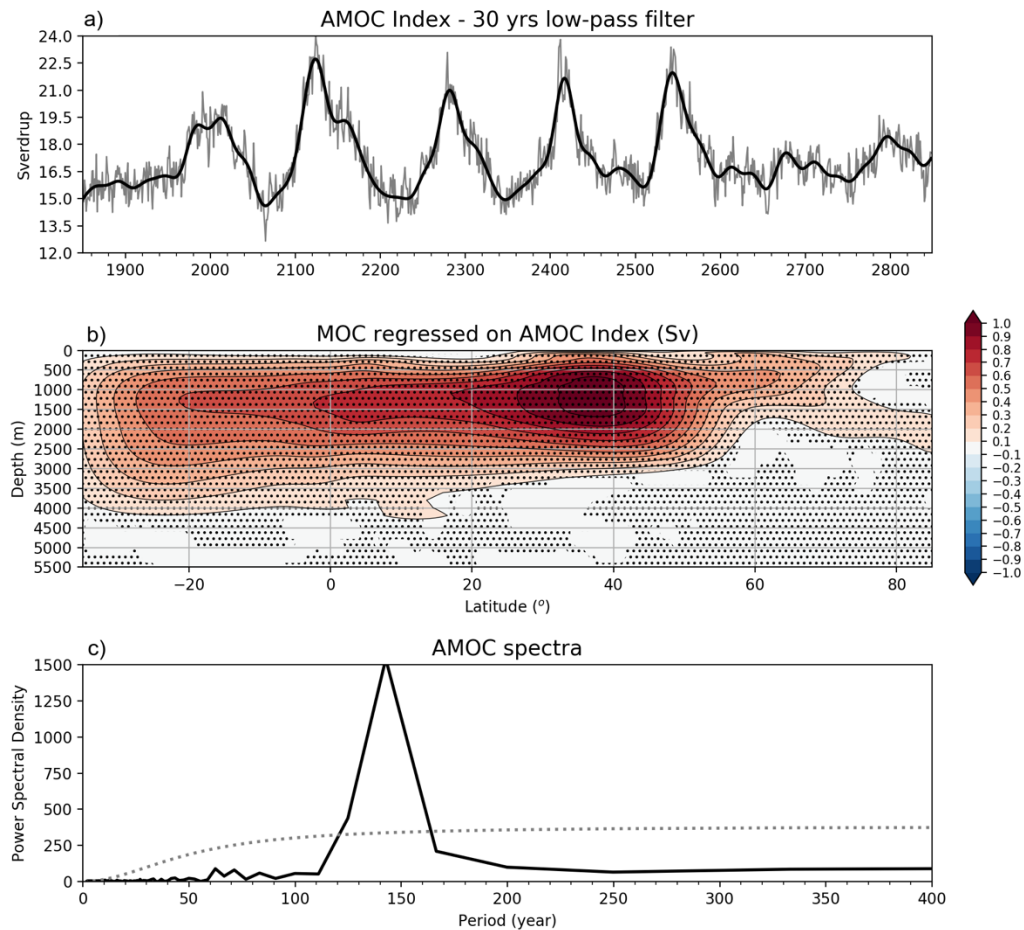


Figure 5: a) timeseries of annual AMOC index (grey) and low-frequency AMOC index (black). b) Atlantic meridional streamfunction regressed on the AMOC index. c) power spectral density of the AMOC index. Significance at 95% confidence level in b) and c) is indicated by dots.

This centennial to multi-centennial oscillation involves the whole Atlantic basin (Fig. 5b); the highest values of meridional streamfunction regressed on the AMOC index are between 30°N and 50°N at around 1000 m depth, in agreement with the AMOC index definition. Since the ocean sets the boundary conditions to the atmosphere through the sea surface temperature, the oceanic low-frequency internal variability has implications for the atmosphere. Because the AMOC is associated with a northward heat transport, the near-surface air temperature is warmer during the strong phase, particularly north of 20°N. The difference in the air temperature between strong and weak phases of the AMOC is larger in boreal winter (not shown), with values higher than 10 degrees in the sub-polar gyre and the GIN seas, which may be linked to the intensified deep convection. The Arctic and Scandinavia warm 2 to 3 degrees and Europe 1 to 2 degrees during the strong AMOC phase with respect to the weak one.

We found that the build-up of salinity anomalies in the Arctic and their subsequent release into the North Atlantic affects the area of deep-water formation and modulates AMOC variability on centennial timescales. Specifically, a strong AMOC effectively transports heat into the high latitudes

of the North Atlantic, favouring the sea-ice melting in the North Atlantic and Arctic, particularly around Greenland and north of Svalbard. The upper-layer salinity and consequently the density in the Arctic reduces. A reduced density yields a high sea surface height and an anticyclonic circulation, trapping the salinity anomaly inside the Arctic and delaying its release into the North Atlantic. As a combination of the resulting circulation and the low sea-ice thickness in the Fram Strait, freshwater slowly exits the Arctic as liquid transport into the GIN seas. This input of freshwater into the GIN seas stabilises the water column that inhibits the deep-water formation, and as a consequence, the AMOC reduces. A weak AMOC transports less heat to the North Atlantic, constraining the sea-ice melting and producing a positive salinity anomaly in the Arctic. This reverts the circulation, and the opposite phase of the cycle starts (Meccia et al., under review).

We have recently found that the above-described 150-year ocean internal variability is not present under conditions of a warmer climate. To study this, we have analysed a set of simulations in which we fixed external forcing conditions corresponding to the years 1990 (*b990*), 2025 (*b025*), 2050 (*b050*) and 2100 (*b100*). In particular, with the computing resources of the third year of this SP, we run *b050*, analysed in detail in Meccia et al. (under review). The 500-year timeseries and power spectral density of the AMOC index for the above-mentioned simulations and 500 years of the *piControl* are plotted in Fig. 6.

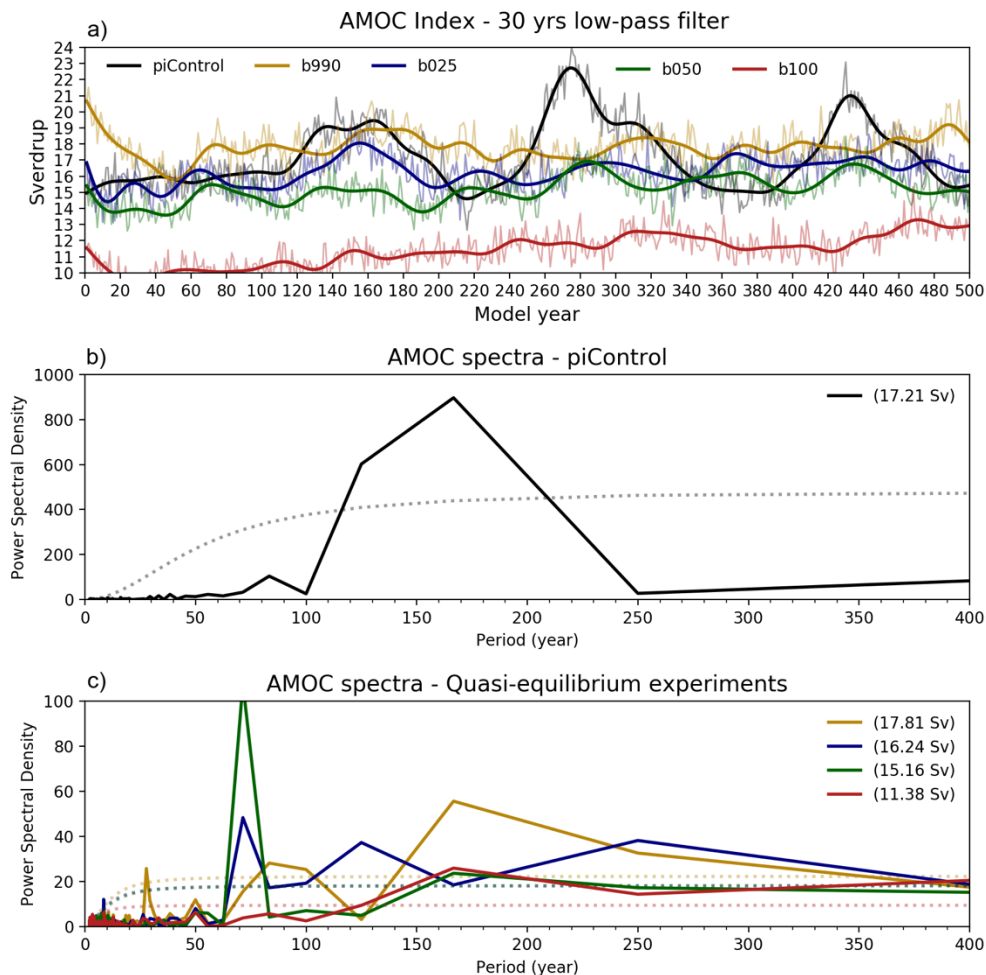


Figure 6: a) annual (thin lines) and 30 year low-pass filtered (thick lines) AMOC index for the first 500 years of *piControl* (black), *b990* (brown), *b025* (blue), *b050* (green) and *b100* (red), representing different quasi-equilibrium climates. b) power spectral density of the AMOC index for the first 500 years of *piControl*. c) power spectral density of the AMOC index for *b990* (brown), *b025* (blue), *b050* (green) and *b100* (red). Significance at 95% confidence level in b) and c) is indicated by dots. The mean values of the AMOC index for each run is displayed between brackets in b) and c).

Although 500 years is a short period for reaching equilibrium in the deep ocean, two main features emerge from Fig. 6. On the one hand, the mean AMOC index value decreases with warming under the SSP5.85 future scenario being 17.21 Sv in the *piControl* run and 15.16 in *b050*. On the other hand, it is notable that the multi-centennial variability in the pre-industrial climate tends to disappear in a warmer climate. There is still a signal in *b990*, but it is very much lower than in the *piControl* run. For *b025* and *b050* experiments, the power spectral density for the multi-decadal variability dominates. Interestingly, the multi-decadal variability disappears in the *b100* integrations. We further analyse *b050* to explain the reduction or even absence of multi-centennial variability in a warmer climate.

The mixed layer depth in March regressed on the AMOC index for the *b050* experiment (Fig. 7b) clearly shows the lack of signal in the GIN seas, at least at lag 0. The maximum value of the mixed layer depth in March obtained in the GIN seas is around 350 m (Fig. 7c), half of the maximum value in the *piControl* run (about 700 m, not shown), and only a slightly significant regression results for lag around 13 years (Fig. 7d). The area of deep convection seems to shift north-eastwards, and values up to 100 m appear to the north of Svalbard. The Labrador Sea remains a region of deep water formation, although it is shifted towards the west (Fig. 7b) with respect to the *piControl* run. However, the deep convection events are weak, with maximum values of MLD in March of 200 m (Fig. 7e), compared to 600 m obtained in the *piControl* run (not shown). The lower values of MLD obtained in the *b050* simulation with respect to the *piControl* are associated with less intense deep convective events explaining why the mean AMOC values are lower.

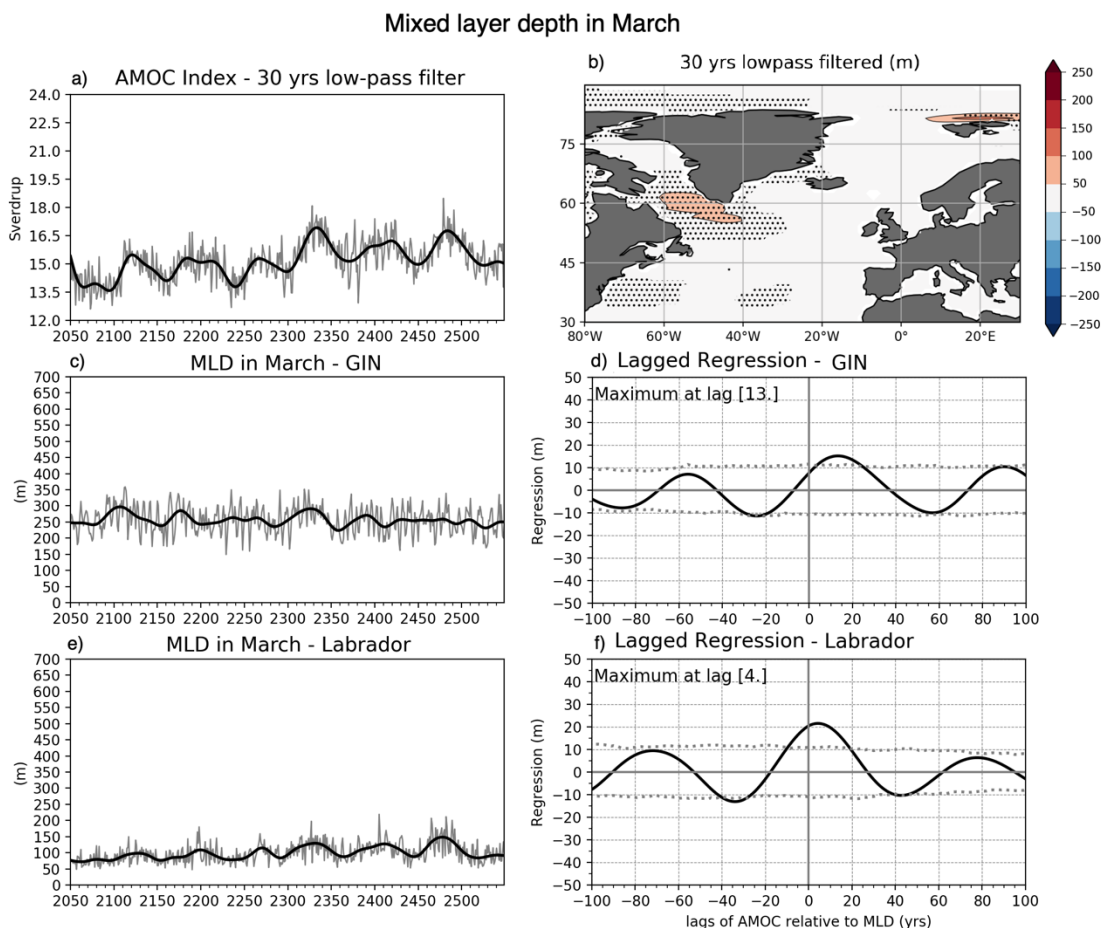


Figure 7: a) timeseries of AMOC index for the *b050* experiment. b) low-frequency MLD (m) in March in the North Atlantic regressed on the AMOC index. c) and e) timeseries of the mean MLD in March in the GIN and Labrador seas, respectively. d) and f) lagged regressions between the AMOC index and the MLD in March in the GIN and Labrador seas. The regressions plotted in the right column are computed after linearly detrending the timeseries. Positive lags indicate that MLD leads AMOC. Negative lags indicate that AMOC leads MLD. Dots in b) and dotted lines in d) and f) show the significance at a 95% confidence level.

In the *piControl* run with a mean AMOC index of  $\sim 17.5$  Sv, the multi-centennial oscillation has a period of around 150 years and an amplitude of 6 Sv approximately (from crest to trough). However, in a warmer climate, the water column in the regions of deep-water formation in the North Atlantic tends to stabilize. As a consequence, the AMOC is expected to reduce. Further, sea-ice cover and sea-ice thickness in the GIN seas and around Greenland and Svalbard are very sensitive to warming. Sea ice tends to disappear in a future scenario with a mean surface air temperature about 4.5 degrees warmer than in the pre-industrial period. Moreover, the mean upper-layer salinity in the Arctic shows larger spatial gradients and consequently stronger mean currents in a warmer climate. Hence, the necessary conditions for maintaining the multi-centennial fluctuations, namely the solid freshwater transport through Fram Strait and the delayed release of the freshwater by liquid transport through the Fram Strait, tend to dissipate with warming.

These results of section b) are under review on Climate Dynamics, and the SP SPITMECC was acknowledged (Meccia et al., under review).

### ***References***

- Meccia V.L., Fuentes-Franco R., Davini P., Bellomo K., Fabiano F., Yang S. and von Hardenberg J. Internal multi-centennial variability of the Atlantic Meridional Overturning Circulation simulated by EC-Earth3, under review on Climate Dynamics.

## List of publications/reports from the project with complete references

### a) Peer-reviewed journals

- Meccia V.L., Fabiano F., Davini P. and Corti S. (2020). Stochastic parameterizations and the climate response to external forcing: An experiment with EC-Earth. *Geophysical Research Letters*, 47, e2019GL085951. <https://doi.org/10.1029/2019GL085951>

Note: The above cited paper was selected to be featured as a Research Spotlight:

- Stanley, S. (2020), An element of randomness in modeling Arctic ice cover, *Eos*, 101, <https://doi.org/10.1029/2020EO142715>. Published on 14 April 2020.
- Meccia V.L, Fuentes-Franco R., Davini P., Bellomo K., Fabiano F., Yang S. and von Hardenberg, J. (2022). Internal multi-centennial variability of the Atlantic Meridional Overturning Circulation simulated by EC-Earth3. *Climate Dynamics*, under review.

### b) International conferences:

- Meccia V., Fabiano F. and Corti S. (2019). Do stochastic parameterizations modify the climate response to external forcing? An experiment with EC-Earth. [Final paper number, A31T-2840] Fall Meeting, *American Geosciences Union*.
- Meccia V., Fabiano F., Corti S. and Davini P. (2019). Arctic sea-ice evolution in EC-Earth 3.1 simulations: sensitivity to Stochastic Physics. *EC-Earth Meeting*, 21-23 May 2019, ECMWF, Reading, UK.
- Meccia V., Fabiano F. and Corti S. (2019). Impact of stochastic physics on climate simulations with EC-Earth: looking at the ocean. Oral presentation. *Geophysical research abstracts Copernicus GmbH*, Vol. 21, EGU2019-18332, 1 pp. Electronic ISSN: 1607-7962; Printed ISSN: 1029- 7006. European Geosciences Union.
- Meccia V., Fabiano F. and Corti S. (2019). Impact of stochastic physics on climate simulations with EC-Earth: looking at the ocean. Poster. *CMIP6 Model Analysis Workshop*, 25-28 March 2019, Barcelona.
- Fabiano F., Meccia V. and Corti S. (2019). Impact of stochastic physics on climate simulations with EC-Earth: looking at the atmosphere. Poster. *CMIP6 Model Analysis Workshop*, 25-28 March 2019, Barcelona.

## Future plans

(Please let us know of any imminent plans regarding a continuation of this research activity, in particular if they are linked to another/new Special Project.)

Regarding the inclusion of SPS in EC-Earth, we are still investigating more in detail the implications on the climate sensitivity and the feedback mechanisms. Regarding the quasi-equilibrium climate under warmer conditions with respect to the pre-industrial ones, we are still studying the changes in the internal climate variability. For the moment, I don't plan to run new simulations.